





Coexistence of insulating phases in confined fermionic chains with a Wannier-Stark potential

N. Aucar Boidi ^{1,*}, K. Hallberg ^{1,2,†}, Amnon Aharony ^{3,‡} and Ora Entin-Wohlman ^{3,§}¹*Centro Atómico Bariloche, Instituto Balseiro, 8400 Bariloche, Argentina*²*Instituto de Nanociencia y Nanotecnología CNEA-CONICET, 8400 Bariloche, Argentina*³*School of Physics and Astronomy, Tel Aviv University, Tel Aviv 6997801, Israel*

(Received 22 September 2023; revised 19 December 2023; accepted 19 December 2023; published 12 January 2024)

We study fermions on a finite chain, interacting repulsively when residing on the same and on nearest-neighbor sites, and subjected to a Wannier-Stark linearly varying potential. Using the density matrix renormalization-group numerical technique to solve this generalized extended Hubbard model, the ground state exhibits a staircase of (quasi) plateaus in the average local site density along the chain, decreasing from being doubly filled to empty as the potential increases. These “plateaus” represent locked-in commensurate phases of charge density waves together with band and Mott insulators. These phases are separated by incompressible regions with incommensurate fillings. These results differ from the many-body localization proposed for this model earlier. It is suggested that experimental variations of the slope of the potential and the range of the repulsive interactions will produce such a coexistence of phases which have been individually expected theoretically and observed experimentally for uniform systems.

DOI: [10.1103/PhysRevB.109.L041404](https://doi.org/10.1103/PhysRevB.109.L041404)

Introduction. The complexity of quantum many-body systems originates from the interplay of strong interactions, quantum statistics, and a large number of quantum-mechanical degrees of freedom. A paradigmatic model, that includes itinerant electrons subject to local and nearest-neighbor (NN) Coulomb interactions, is the extended Hubbard model (EHM), which leads to interesting features like metal to insulator transitions, charge and spin density waves, and other interesting phases. In one dimension [1–5], it has also been used to describe data collected in experiments performed on chains of cold atoms [6,7]. In higher dimensions, it has been used to describe bulk and edge states in electronic insulators [8].

Experiments on cold-atom arrays naturally involve finite samples. Numerical calculations performed on such systems used various boundary conditions: hard walls, periodic and open boundaries, or potentials representing confining harmonic traps [7,9,10]. These papers concentrate mostly on the region around the “center” of the confined structure, whose details are usually not sensitive to the particular form of the boundaries, and so its possible structures are determined by the local and interactions and by the average particle density n . Remarkably, experiments (e.g., on cold atoms) have observed some of the theoretically predicted phases [11,12]. Less attention has been paid to the structures near the “edges” of the samples and to their dependence on the details of the boundary conditions, in particular when the confinement is achieved by varying site energies. Such a confining scheme has been recently considered, using the self-consistent Hartree-Fock

approximation, for the two-dimensional EHM, and found coexistence of various structures (phases) near the free ends of the samples [8].

One way to model the edges of such finite systems uses a linear confining potential, which grows as one moves away from the bulk [8]. In fact, such a linear potential is the same as the Wannier-Stark potential, which arises due to a constant electric field along the one-dimensional chain. For single electrons, this potential generates a ladder of localized states, which were predicted to remain (many-body) localized also with interactions. [13] Indeed, recent experiments found a coexistence of localized and weakly localized phases on 1D finite-sized mosaic Wannier-Stark photonic lattices [14].

In this Letter, we generalize the EHM to a 1D fermionic chain, confined by a *linear potential*, which mimics either edge configurations in bulk systems or cold-atom arrays placed in an electric field. Such a potential can be produced by a longitudinal electric field, as in the Wannier-Stark model [15].

Given the complex nature of the many-body problem associated with our system, we resort to one of the most accurate numerical methods for correlated systems, the density matrix renormalization group (DMRG) [16–21], which uses quantum information to keep the most relevant states. As we show, the linear potential generates in the ground state the simultaneous existence of segments in which different phases coexist, each of which having been observed separately before, on long uniform chains. This coexistence of phases differs from the many-body localized states proposed earlier [13–15]. This apparent contradiction is one of our main results.

Our results are presented by plots of the local quantum-averaged density on the sites i on the chain, $\langle n_i \rangle$, the NN density-density correlations $\langle n_i n_{i+1} \rangle$ and the NN spin-spin correlations $\langle s_i^z s_{i+1}^z \rangle$, (e.g., Fig. 2). Instead of a smooth decrease, the local average of $\langle n_i \rangle$ shows flat steps, corresponding to locked-in Mott or CDW structures (e.g.,

*nairaucar@gmail.com

†karenhallberg@gmail.com

‡aaharonyaa@gmail.com

§orawohlman@gmail.com

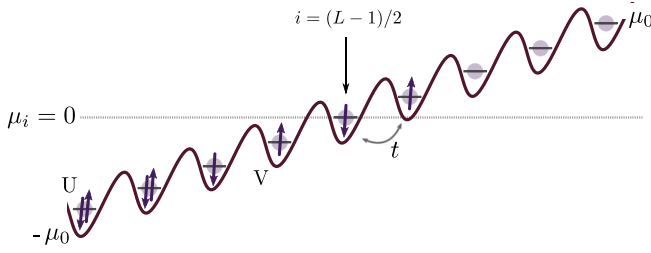


FIG. 1. Schematic representation of the system considered.

212121 ..., 101010 ..., [22]). These locked-in steps are similar to those observed for commensurate wave vectors in the devil's staircase (see Refs. [23,24] for the physical description of these terms). Unlike all the previous cases, in which such lock-ins occur in momentum space, here we find them in real space.

Between these steps, $\langle n_i \rangle$ decreases more smoothly, representing incommensurate regions, which can be thought of as “domain walls” with varying lengths [25]. As shown below, the local density of states on these intermediate sites exhibits small energy gaps, which imply that they are incompressible (insulating), in spite of having incommensurate fillings, which could be due to Wannier-Stark localization [26] and which deserve further study. We will refer to them hereafter as incompressible incommensurate-filling phases “IIF.” In this paper, we find a coexistence of all these phases on one single sample, e.g. band and Mott insulators, charge density waves with different mean fillings, and gapped incommensurate filling phases separating these regions.

The specific sequence of phases, and their sizes, can be modified experimentally, e.g., by changing the slope of the potential. Neighboring structures in a sequence are often also neighboring in the phase diagrams found for uniform systems (which are not subjected to the linear potential).

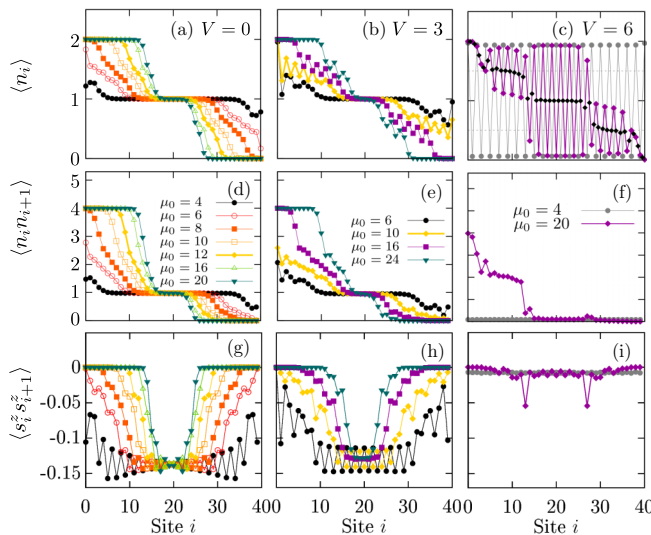


FIG. 2. [(a)–(c)] The local density $\langle n_i \rangle$; [(d)–(f)] the NN density-density correlations $\langle n_i n_{i+1} \rangle$; [(g)–(i)] the NN spin-spin correlations $\langle s_i^z s_{i+1}^z \rangle$, for $V = 0, 3, 6$ and different values of μ_0 . The black diamonds in (c) indicate the mean value between neighboring sites.

Model. We study the generalized 1D EHM Hamiltonian

$$\begin{aligned} \mathcal{H} = & -t \sum_{i,\sigma} (c_{i,\sigma}^\dagger c_{i+1,\sigma} + \text{H.c.}) + \sum_i (\mu_i - \mu) n_i \\ & + U \sum_i (n_{i,\uparrow} - 1/2)(n_{i,\downarrow} - 1/2) \\ & + V \sum_i (n_i - 1)(n_{i+1} - 1), \end{aligned} \quad (1)$$

where i is the site index, $i = 0, \dots, L-1$. [27] Here, μ is the fixed external chemical potential, $c_{i,\sigma}^\dagger$ creates an electron with spin $\sigma (= \uparrow, \downarrow)$ at site i , $n_{i,\sigma} = c_{i,\sigma}^\dagger c_{i,\sigma}$, $n_i = n_{i,\uparrow} + n_{i,\downarrow}$, while U and V are the repulsive interactions between electrons on the same and NN sites, respectively (see Fig. 1). The figure also shows the gradual decrease of the local occupation as the confining potential increases from left to right. The site-dependent local energy (the Wannier-Stark potential) μ_i describes a linear external potential, $\mu_i = \mu_0[i/i_c - 1]$. The site $i_c = (L-1)/2$ represents the center of the “edge,” where $\mu_{i_c} = 0$. The particular form of \mathcal{H} was chosen so that at $\mu = 0$ (up to a constant energy) it is particle-hole symmetric when $i \rightarrow L-1-i$ and $n_i \rightarrow 2-n_i$. In that case, we always have $n_{i_c} = 1$.

For an infinite chain, μ_i is large and negative at large and negative i , and therefore we expect all the sites there to be filled, i.e., $n_i = n_{i,\uparrow} + n_{i,\downarrow} = 2$. Similarly, μ_i is large and positive at large and positive i , and therefore we expect all the sites there to be empty, i.e., $n_i = 0$. For a finite chain, as we use here, this is still expected for a large slope, $\mu_0 \gg 1$, when the whole “edge” between the fully occupied and empty “phases” is confined within the chain. Indeed, this is confirmed by our calculations. However, the “end” trivial phases disappear for small slopes, for which the observed structures depend on the open boundaries.

Results. We have used wide ranges for the parameters, such that all the interesting structures appear in the resulting phase diagrams. Unless otherwise stated, we use $U/t \rightarrow U = 10$, $\mu = 0$, and $L = 41$. All energies are measured in units of t . The Hamiltonian is diagonalized exploiting the DMRG technique, with around $m = 500$ states and 4 to 6 finite-size sweeps, which leads to a precision of around 10^{-10} in the energy. For a very steep potential ($\mu_0 \rightarrow \infty$), we obtain only two coexisting “phases”: a completely filled band ($n_i = 2$) up to the center point i_c , and completely empty sites ($n_i = 0$) above that point, as expected. Both regions are incompressible and insulating. As the slope μ_0 decreases (but remains large), these two “phases” remain near the two ends of the system, but new structures (“phases”) appear between them, in which $\langle n_i \rangle$ decreases gradually from 2 to 0. Figure 2 presents typical results, for three values of V . Note the electron-hole symmetry between the two sides of Figs. 2(a)–2(c), which follows directly from Eq. (1) at $\mu = 0$.

For $V = 0$ (i.e., the simplest Hubbard Hamiltonian, left column in Fig. 2), the system shows the following phases: for large (but finite) values of μ_0 , it is a band insulator at both extremes, completely filled on the left and completely empty on the right. In the region located symmetrically around the center point i_c , we find a Mott-insulating state (one particle per site, $\langle n_i \rangle = 1$), and an antiferromagnetic spin-spin correlation

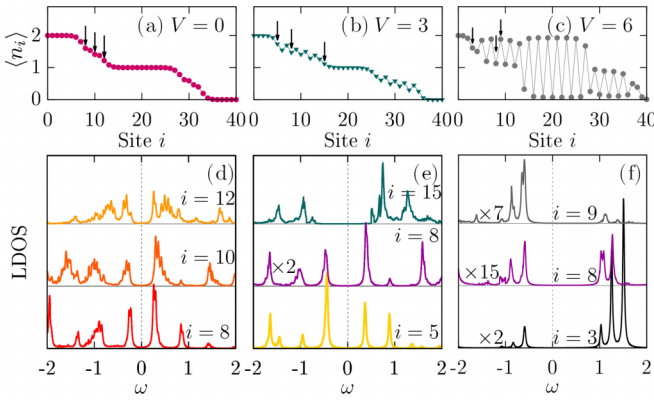


FIG. 3. (Top) Local density profile $\langle n_i \rangle$ showing the sites where the local density of states (LDOS) has been calculated, for $V = 0$ ($\mu_0 = 10$), $V = 3$ ($\mu_0 = 16$), and $V = 6$ ($\mu_0 = 20$). (Bottom) LDOS showing gaps at the Fermi energy (at $\omega = E_F = 0$) for all cases, using $\eta = 0.01$ (Eq. (S1) in Ref. [30]).

function, Fig. 2(g). As seen in this figure, the spin correlation function, $\langle s_i^z s_{i+1}^z \rangle \simeq -0.14$ (note: $s_i^z \equiv (n_{i,\uparrow} - n_{i,\downarrow})/2$, the z -direction is arbitrarily chosen), agrees with its value of the infinite Mott phase. [17,28] The three insulating commensurate phases are separated by IIF regions with very small but finite gaps, see Fig. 3. These regions differ from the compressible regions found in Ref. [8], possibly because Ref. [8] explores 2D systems using the mean-field approximation. As μ_0 decreases, the band insulating phases on both ends disappear and the Mott region grows, as estimated below. These results are also consistent with the behavior of the density-density correlations, which vary between 4 on the left, via 1 in the Mott phase, to 0 on the right, Fig. 2(d).

For $V = 3$ (middle column in Fig. 2), the above three insulating “phases” are supplemented by two regions with an incipient (doped) CDW order on the two sides of the Mott “phase,” with local mean fillings “quasiplateaus” around $\langle n_i \rangle \simeq 1.5$ and $\langle n_i \rangle \simeq 0.5$ (quarter filling of holes and of electrons, respectively). The bar indicates a local average over a few sites. Unlike the uniform case $\mu_i = 0$, the local average fillings in these regions are not exactly 1.5 and 0.5. Rather, they can be fitted by $\langle n_i \rangle = A - Bi + C \cos(i\pi)$ (note that i is the site number!). The oscillating term corresponds to a CDW, with a wave vector $q = \pi$ (our lattice constant is 1) and structures 212121... or 101010... [22]. However, the term $-Bi$ represents a linear decrease of the actual average, presumably in response to the linear potential. Without this linear “background,” such a CDW is consistent with the results of the density-density and spin-spin correlations and with previous results for the doped (non-half-filled) 1D EHM [29] in a uniform potential, $\mu_i = 0$, for which there is a transition from a Tomonaga-Luttinger liquid to a CDW phase for intermediate values of $2t \leq V < U/2$ and large values of U ($U \gg t$). In those cases this CDW phase is insulating and incompressible. As we discuss below, we also find that, in spite of the varying average local densities, the local density of states has a (small) gap at the Fermi energy, which is consistent with an incompressible state. These regions may become compressible at low finite temperatures, which may be very different from the corresponding charge density

phases for a uniform system with a fixed average occupation. As before, when μ_0 decreases, the Mott region grows, the incipient CDW regions move towards the boundaries and the band-insulating regions disappear.

For $V = 6$ (right column in Fig. 2), the Mott region disappears and is replaced by a half-filled CDW, 202020... For large μ_0 's, this phase exists in the center and coexists with doped CDW's at both sides, with fillings $\langle n_i \rangle \simeq 1.5$ and $\simeq 0.5$, respectively [black diamonds in Fig. 2(c)]. This coexistence of two different CDW's has not been seen before and constitutes a situation which could be observed in cold-atom experiments. As before, the doped CDW's are accompanied by a very small gradual decrease of the local average occupation -‘quasiplateaus’, presumably due to the slope in the potential. When μ_0 is lowered, the half-filled CDW occupies the whole chain. This is expected, since it is well known that when $V > U/2$ and for a half-filled system, the uniform chain undergoes a transition from a Mott phase to a CDW [5,29]. The results are consistent with the behavior of the density-density and spin-spin correlations. It is interesting to see a finite value of the spin-spin correlations at the phase boundaries between the half-filled and doped CDW's. It is also interesting to see that for $V = 3$ the average occupation $\langle n_i \rangle$, and the amplitude of the incipient CDW decrease gradually towards the central Mott or CDW region, but this decrease becomes abrupt for $V = 6$. The width of the IIF region (domain wall) between the two CDW phases seems to shrink to zero above some “critical” value of V .

The above results exhibited “plateaus” only for 1/2, 1/4, and 3/4 fillings. We expect similar “plateaus,” corresponding to other simple fraction, e.g., 1/8. However, to see these one would need a much larger number of sites, and this is not possible with our present computer capabilities. Note, though, that calculations with a smaller number of sites do still show similar steps for these commensurate fillings.

Local density of states. To further explore the different phases, we have calculated the local, site dependent, density of states (LDOS), using the lesser and greater Green's functions, see details in Ref. [30]. In Fig. 3, we show the LDOS for particular sites of the chain for different parameters. We observe that there is always a gap at $E_F = 0$, even for the partially filled sites (we have added the filling profile for comparison). The gaps corresponding to these sites are smaller than the corresponding gaps of the fully formed CDW (see the $V = 6$ case) and much smaller than those of the Mott region (see Fig. 4). These gaps indicate that these regions are incompressible (nonmetallic). This is not a finite size effect (since we would have a finite LDOS at E_F for fractional densities), but a consequence of the linear potential. We also observe that the LDOS consists of a series of peaks separated by minigaps, a possible indication of Stark discretization [15].

Figure 4 shows a heatmap of the local density of states along the chain for $V = 0$, $\mu = 0$ and $\mu_0 = 10$. The Fermi energy is marked by a white (dashed) line at $\omega = 0$. As the Hamiltonian is particle-hole symmetric around the middle of the chain, the density of states for the right half of the chain ($20 \leq i \leq 40$, not shown) is inverted as a function of ω (details see in Ref. [30]). As mentioned above (Fig. 3), we always find a gap at E_F , indicating an incompressible state. This gap is more than an order of magnitude smaller than the Mott gap. We also see a structure in the Hubbard bands in the

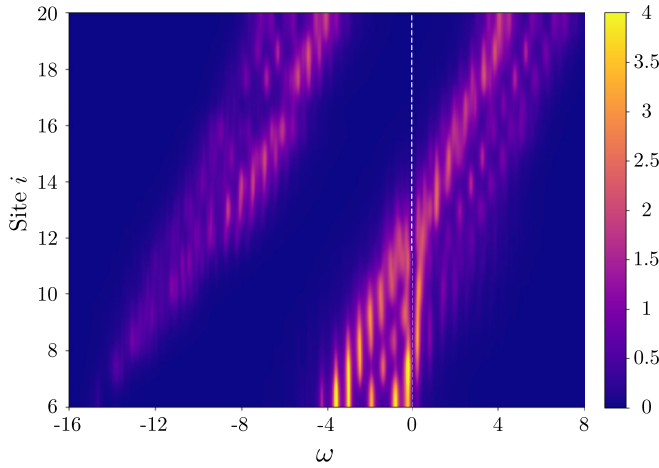


FIG. 4. Heat plot of the local density of states at different sites ($6 \leq i \leq 20$) for $\mu_0 = 10$ and $V = 0$. The Fermi energy is marked by a white (dashed) line at $\omega = 0$.

form of three main substructures which evolve along the chain sites. Each substructure extends to around three neighboring sites, also an indication of Stark localization which requires future study [15].

An interesting result for $V = 0$ is the existence of a (negative) high-energy localized state in the IIF region (clearly seen in the density of states plots at the left of the chain, Fig. S3 in Ref. [30]). We can see a small and narrow peak at energies around $\omega \sim -14$ for the first sites of this region, which evolves to higher energies (following the increase of μ), while we approach the Mott region, increasing its width. This state is reminiscent of the lower Hubbard band for the left regions. A similar state is seen for the right half of the chain which is reminiscent of the upper Hubbard band (not shown). More results for the density of states, together with some calculations in the atomic limit, are presented in Ref. [30].

Size of the Mott region. At the electron-hole symmetric case (and $V = 0$), the upper and lower Hubbard bands are centered at $\pm U/2$ respectively, each with a total width of 4. For $\mu = 0$, the size of the Mott region can be estimated recalling that the Mott insulating state requires that the local μ_i lies within the Mott gap, i.e., $-U/2 + 2 < \mu_i < U/2 - 2$. At the lower limit $\mu_{\min} = -U/2 + 2$, yielding that $i_{\min}\mu_0 = i_c(\mu_0 - U/2 + 2)$, while at $\mu_{\max} = U/2 - 2$ one finds $i_{\max}\mu_0 = i_c(\mu_0 + U/2 - 2)$. Consequently, assuming that the width of the Hubbard bands is not modified by the presence of the confining potential, the size of the Mott region is

$$L_{\text{Mott}} = i_{\max} - i_{\min} = (U/2 - 2)(L - 1)/\mu_0. \quad (2)$$

As the confining potential slightly increases the width of the Hubbard bands (not shown), the gap in-between them and L_{Mott} are slightly overestimated.

To compare Eq. (2) with our numerical results, we have estimated the size of the Mott region by defining its boundaries at the points where the linear fits of the numerical derivative of the local occupation intercept 0 for each value of μ_0 , using the results shown in Fig. 2(a). This procedure reveals that indeed

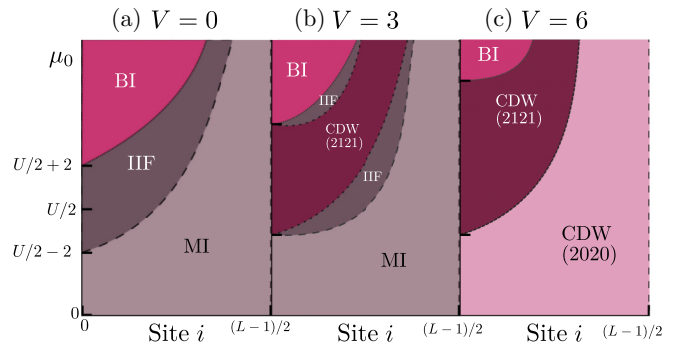


FIG. 5. Schematic plot of the various phases observed in the chain subjected to a linear potential, for three different regimes defined by the nearest-neighbor interaction V . The sequence of numbers, 212121 and 202020, refer to the occupations of neighboring sites. MI: Mott insulator, BI: band insulator, IIF: incompressible incommensurate-filling phase.

the size of the Mott region is proportional to $1/\mu_0$ (see Fig. S2 in Ref. [30]), and it shrinks to zero for very steep potentials.

Changing the global chemical potential. Changing the global chemical potential simply shifts the site at which the linear potential vanishes to $i_c^{\text{shift}} = i_c(1 + \mu/\mu_0)$. For the infinite chain, this results by a simple shift of all the phases in Fig. 2, along the chain, with no other change. The same happens for finite chains with a large slope, when i_c^{shift} remains far from the boundaries of the chain. Otherwise, the structure changes near the boundaries, see Fig. S5 in Ref. [30].

Discussion. In this paper, we study the one-dimensional extended Hubbard model, subject to a linearly varying Wannier-Stark potential on a finite chain, applying the density-matrix renormalization group. We find an interesting sequence of several insulating electronic phases in the ground state, in which regions with commensurate charge density waves coexist with band and Mott insulating phases. These regions are separated by incompressible domain walls with incommensurate fillings, which were not reported before. The results are summarized in Fig. 5. Further research is needed to define whether these incompressible walls are due to the Stark many-body localization [26]. The steeper the slope of the external potential, the narrower the domain walls. These phases and domain walls can be moved around by varying a global chemical potential, thus, providing a possible functionality of this kind of systems. Cold-atom chains placed in an external electric field are suggested as experimental realizations of our system.

Finally, although our accurate results are similar to those found approximately in Ref. [8] for the edges of two-dimensional samples, there remain several important differences, e.g., concerning the compressibility and conductance of the intermediate phases. If the gaps we find persist to two dimensions, those edges will become insulating at zero temperature. Repeating our calculations for the two-dimensional case may resolve these differences, and yield important information on the edge states of topological systems.

Acknowledgments. N.A.B. and K.H. acknowledge support from ICTP through the STEP and Associates Programmes respectively, and from the PICT 2018-01546 grant of the ANPCyT. The authors thank useful discussions with Carlos Balsero.

- [1] T. Giamarchi, Mott transition in one dimension, *Physica B: Condens. Matter* **230**, 975 (1997).
- [2] F. Mila and X. Zotos, Phase diagram of the one-dimensional extended Hubbard model at quarter-filling, *Europhys. Lett.* **24**, 133 (1993).
- [3] Y. Z. Zhang, Dimerization in a half-filled one-dimensional extended Hubbard model, *Phys. Rev. Lett.* **92**, 246404 (2004).
- [4] S. Ejima and S. Nishimoto, Phase diagram of the one-dimensional half-filled extended Hubbard model, *Phys. Rev. Lett.* **99**, 216403 (2007).
- [5] S. Glocke, A. Klümper, and J. Sirker, Half-filled one-dimensional extended Hubbard model: Phase diagram and thermodynamics, *Phys. Rev. B* **76**, 155121 (2007).
- [6] I. Bloch, J. Dalibard, and W. Zwerger, Many-body physics with ultracold gases, *Rev. Mod. Phys.* **80**, 885 (2008).
- [7] X. W. Guan, M. T. Batchelor, and C. Lee, Fermi gases in one dimension: From Bethe Ansatz to experiments, *Rev. Mod. Phys.* **85**, 1633 (2013).
- [8] U. Khanna, Y. Gefen, O. Entin-Wohlman, and A. Aharony, Edge reconstruction of a time-reversal invariant insulator: Compressible-incompressible stripes, *Phys. Rev. Lett.* **128**, 186801 (2022).
- [9] A. Recati, P. O. Fedichev, W. Zwerger, and P. Zoller, Spin-charge separation in ultracold quantum gases, *Phys. Rev. Lett.* **90**, 020401 (2003).
- [10] F. Heidrich-Meisner, G. Orso, and A. E. Feiguin, Phase separation of trapped spin-imbalanced Fermi gases in one-dimensional optical lattices, *Phys. Rev. A* **81**, 053602 (2010).
- [11] M. Boll, T. A. Hilker, G. Salomon, A. Omran, J. Nespolo, L. Pollet, I. Bloch, and C. Gross, Spin- and density-resolved microscopy of antiferromagnetic correlations in Fermi-Hubbard chains, *Science* **353**, 1257 (2016).
- [12] D. Greif, M. F. Parsons, A. Mazurenko, C. S. Chiu, S. Blatt, F. Huber, G. Ji, and M. Greiner, Site-resolved imaging of a fermionic Mott insulator, *Science* **351**, 953 (2016).
- [13] D. O. Krimer, R. Khomeriki, and S. Flach, Delocalization and spreading in a nonlinear Stark ladder, *Phys. Rev. E* **80**, 036201 (2009); R. Khomeriki, D. O. Krimer, M. Haque, and S. Flach, Interaction-induced fractional Bloch and tunneling oscillations, *Phys. Rev. A* **81**, 065601 (2010).
- [14] J. Gao, I. M. Khaymovich, A. Iovan, X.-W. Wang, G. Krishna, Z.-S. Xu, E. Tortumlu, A. V. Balatsky, V. Zwiller, and A. W. Elshaari, Coexistence of extended and localized states in finite-sized mosaic Wannier-Stark lattices, *Phys. Rev. B* **108**, L140202 (2023).
- [15] M. Udono, T. Kaneko, and K. Sugimoto, Wannier-stark ladders and stark shifts of excitons in mott insulators, *Phys. Rev. B* **108**, L081304 (2023).
- [16] S. R. White, Density matrix formulation for quantum renormalization groups, *Phys. Rev. Lett.* **69**, 2863 (1992).
- [17] S. R. White, Density-matrix algorithms for quantum renormalization groups, *Phys. Rev. B* **48**, 10345 (1993).
- [18] K. A. Hallberg, New trends in density matrix renormalization, *Adv. Phys.* **55**, 477 (2006).
- [19] U. Schollwöck, The density-matrix renormalization group, *Rev. Mod. Phys.* **77**, 259 (2005).
- [20] U. Schollwöck, The density-matrix renormalization group in the age of matrix product states, *Ann. Phys.* **326**, 96 (2011).
- [21] M. C. Bañuls, Tensor network algorithms: A route map, *Annu. Rev. Condens. Matter Phys.* **14**, 173 (2023).
- [22] The series of numbers represent the average occupations.
- [23] P. Bak, Commensurate phases, incommensurate phases and the devil's staircase, *Rep. Prog. Phys.* **45**, 587 (1982).
- [24] K. Inagaki, K. Nakatsugawa, and S. Tanda, Lock-in transition of the charge-density waves of quasi-one-dimensional conductors: origin of the first-order transition, [arXiv:2304.11525](https://arxiv.org/abs/2304.11525).
- [25] D. Cho, G. Gye, J. Lee, S.-H. Lee, L. Wang, S.-W. Cheong, and H. W. Yeom, Correlated electronic states at domain walls of a Mott-charge-density-wave insulator $1T - \text{TaS}_2$, *Nat. Commun.* **8**, 392 (2017).
- [26] M. Schulz, C. A. Hooley, R. Moessner, and F. Pollmann, Stark many-body localization, *Phys. Rev. Lett.* **122**, 040606 (2019).
- [27] Without loss of generality we consider an odd number of sites, so that the Wannier-Stark potential μ_i is zero at the site located in the middle of the chain. We obtained similar results also for even numbers of sites.
- [28] Due to rotational invariance, the total spin-spin correlation function in this reference is three times the one presented here. The oscillations around this value arise due to the finite size of the sample.
- [29] M. Nakamura, Tricritical behavior in the extended Hubbard chains, *Phys. Rev. B* **61**, 16377 (2000).
- [30] See Supplemental Material at <http://link.aps.org/supplemental/10.1103/PhysRevB.109.L041404> for details.